2018 IEEE 15th International Symposium on Biomedical Imaging (ISBI 2018)
April 4-7, 2018, Washington, D.C., USA

AUTOMATED OVARIAN VOLUME QUANTIFICATION IN TRANSVAGINAL ULTRASOUND

Ravi Teja Narra[⋆]*, Nitin Singhal*[⋆]*, Nikhil S. Narayan*[⋆]*, and Ramaraju GA*[†]*, MD*

[⋆] Samsung R&D Institute India, Bangalore
[†] Krishna IVF Clinic, Visakhapatnam, India

ABSTRACT

Ovarian quantification by volume measurement is performed in routine clinical practice for diagnosis and management of gynecological conditions such as infertility. This paper describes an automated algorithm for ovarian volume measurement using three-dimensional transvaginal ultrasound (TVUS) images. The algorithm integrates deep learned energy map as a soft shape prior within the variational segmentation framework for 2D radial slice segmentation. The output of the segmentation framework is used for mesh generation using U-V spherical parametrization to estimate the surface of the ovarian volume. The segmentation framework provides approximately 86% average Dice overlap with the ground truth annotations. The mean absolute volume difference is found to be approximately 5ml between manual and automated measurements on 55 TVUS images.

***Index Terms*—** Ovary, Ultrasound, Segmentation, U-V parametrization, Deep-Learning

1. INTRODUCTION

Ovary is an organ of the female reproductive system that is responsible for the synthesis of the ovum. The ovum when fertilized develops into an embryo. The size of a normal ovary varies with age and a recent study by Thomas W. Kelsey et al. [1] shows that its size increases until 20 years of age with a gradual decline at the menopause.

Quantification of the ovarian volume plays an important role in the diagnosis and management of gynecological conditions such as infertility. Ovarian volume is a useful indicator of the response to hyper-stimulation in assisted reproduction. It is known that there is a direct correlation between the number of non-growing follicles (NGF) and the ovarian volume [2]. The dosage protocol for initiating hyper-stimulation is determined by estimating the number of NGF based on ovarian volume. The accuracy of the ovarian boundary segmentation directly affects the ovarian volume estimation. Furthermore, the segmented ovarian boundary helps in reducing the false follicle detection and preventing follicle bleeding by reducing the search space in state-of-the-art follicle quantification tools such as 5D Follicle™ [3].

Three-dimensional transvaginal ultrasound (TVUS) is an effective imaging modality for ovarian volume assessment. The acquired TVUS volume is analyzed by clinicians to detect and quantify the ovarian volume. While the evaluation procedure is largely manual, a few medical software and semi-automated methods have been proposed to assist the procedure. VOCAL (Volume Organ Computer-aided AnaLysis) is a state-of-the-art software tool which enables volume measurements by rotating the structure around a fixed axis and manually delineating the 2D slices. The delineation on 2D slices is interpolated to generate a 3D surface representing the ovarian volume. However, VOCAL measurements suffer from following limitations [4]: (1) interpolation errors; (2) overestimation of true anatomical volume; (3) time needed to manually perform the segmentation on 2D slices; and (4) difficulty in identifying structures in presence of shadows. Algorithm frameworks to obtain better segmentation results and recognition rates for ovarian follicles by reducing the search space for follicle detection are presented in [5, 6]. However, their main goal is not to accurately segment the ovarian boundary and volume quantification evaluation is missing.

We hypothesize that automating the quantification of ovarian volume would significantly speed up the clinical workflow, reduce operator bias, and help harness the full potential of TVUS in clinical practice. The main goal of the automated solution is to accurately delineate the ovarian boundary from TVUS volumes.

Traditional variational segmentation frameworks such as Active Contour rely on precise initialization and are susceptible to errors [7, 8]. In recent years, deep learning based fully convolutional network (FCN) have seen application for object detection and localization [9]. However, the performance of these techniques for precise object boundary segmentation is often limited when the training dataset is small and in presence of high structural variability.

In this paper, we propose a segmentation framework, which uses deep learned energy map in the variational energy formulation to segment 2D radial slices extracted from a TVUS image. The segmentation is followed by mesh generation to estimate the surface of the ovarian volume. The proposed algorithm is robust towards initialization errors, boundary leakage at areas of less edge information, compu-

978-1-5386-3636-7/18/$31.00

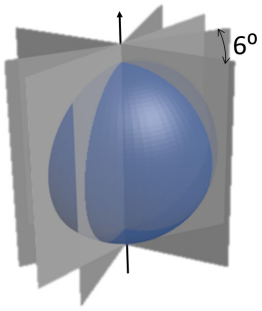

Fig. 1. Radial Slice Extraction

tationally less expensive, and is capable of segmenting the ovarian region to desired accuracy. The methodology and experimental results are discussed in following sections.

2. METHODOLOGY

A series of 2D slices are extracted from the volume by rotational-based slicing technique (see Fig. 1). We use a 6^o separation between slices, which generates 30 radial slices per volume. The segmentation on each 2D radial slice is carried out by a variational energy formulation. The mathematical formulation is presented in the following subsections.

2.1. Segmentation Framework

We present a segmentation framework for accurate 2D radial slice segmentation, which uses a deep learned energy map $P_L : \mathbb{R}^2 - > (0, 1)$. This energy map works as an effective prior for ovarian structure localization. P_L is obtained from a trained FCN described in next subsection. Segmentation is realized within a level set functional by minimizing a cost function. The cost function includes terms for image features (edge) and shape prior, and is formulated as

$$J = J_{image} + \lambda J_{shape}, \tag{1}$$

where,

$$\begin{aligned} J_{image} &= \int_{\Omega} \left(g(|I|)\,|\nabla H(\phi)|\right) d\phi, \\ J_{shape} &= \frac{1}{2} \int_{\Omega} \left(H(\phi) - H(\phi_L)\right)^2 H(\phi) d\phi. \end{aligned} \tag{2}$$

The ovarian boundary is represented by the level set function ϕ, thereby partitioning the image $\Omega \subset \mathbb{R}^2$ into interior and exterior regions. The function $g(|I|) = \frac{1}{1+|\nabla I|}$ is the edge indicator function and assumes a low value at the edge of the image. $H(\phi)$ is the Heaviside function.

The second term in (1), is a soft shape prior which is used to penalize deviation of ϕ from prior term ϕ_L. The prior term

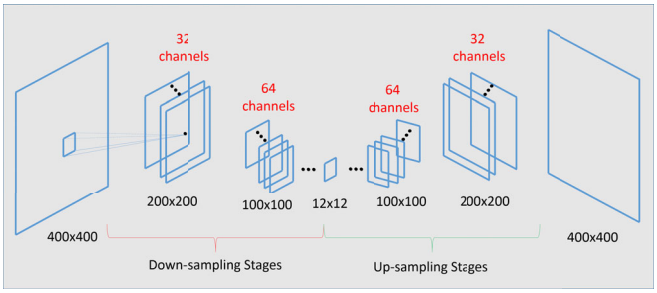

Fig. 2. U-Net architecture used for contour initialization.

ϕ_L is computed as signed distance transform of the binarized deep learned energy map defined as $b(x, y) = 1$ if $P_L > 0.5$ and zero otherwise. In the following subsection, we describe the derivation of P_L.

Deep Learned Prior

A U-Net [10] architecture is used to localize the ovary in 2D radial slices. The network consists of a 5 stage downsampling and 5 stage upsampling branches. At each stage, the input image is downsampled by a factor of 2 using 2x2 convolution/deconvolution operation with stride 2. The architecture (see Fig. 2) predicts the probability of each pixel belonging to ovarian structure in a test slice. During training, the architecture learns the weights at different stages using manually annotated training slices. The learned weights are used to predict and assign a energy map $P_L(x, y)$ to each pixel in a test slice.

2.2. Curve Propagation

Minimizing the cost function in (1), results in curve evolution such that the output level set function ϕ is aligned with the image edges and does not deviate from the learned prior ϕ_L. The cost function is minimized by setting the derivative to zero and solving the resulting Partial Differential Equation (PDE) by using gradient descent and $\phi_0 = \phi_L$. The PDE is presented as

$$\frac{\partial J}{\partial \phi} = \left(div\left(g \frac{\nabla \phi}{|\nabla \phi|} \right) - \lambda (H(\phi) - H(\phi_L)) \right) H^{'}(\phi). \tag{3}$$

However, the above curve evolution suffers from smoothness in areas of less edge information. In order to force smoothness of the curve, a discrete morphological curvature operator, equivalent to the mean curvature motion is used and applied after every N iterations. The morphological operator is given by

$$\phi_{k+1} = (\phi_k \bullet B_d) \circ B_d, \tag{4}$$

where B_d is the binary structuring element, ϕ_k is the curve at kth iteration and $\circ$ is the morphological "open" operator and $\bullet$ is the morphological "close" operator.

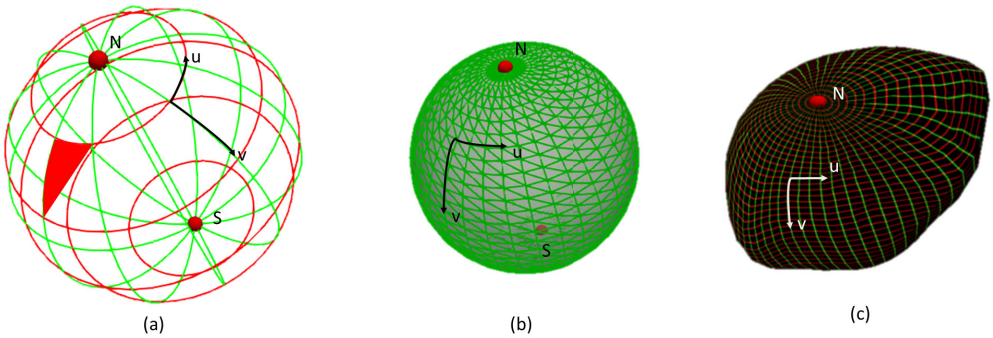

Fig. 3. (a) Spherical model formation using interpolated points. A representative mesh triangle (in red) is shown to describe the triangle generation step. (b) Parametrized spherical model used for ovarian volume representation, where u and v are radial and axial parameters respectively. (c) Smooth 3D mesh structure representing ovarian volume.

2.3. Mesh Generation

A 3D mesh structure is generated using segmented boundary points in every 2D radial slice. Spherical parameterization is used to generate a structured grid $(u, v) : \mathbb{R}^3$.

The parameterization is performed along the U and V directions, with U direction along the latitude on the surface of the ovary and V direction along the segmented boundary contours (ovarian boundary in 2D radial slices) as shown in Fig. 3(a). The parameter value along both the directions are computed based on normalized distance along the respective paths.

The spherical parametrization is directly used for triangle generation. Let the discretized nodes along U and V direction be

$$\begin{aligned} u_i &: i = 0, 1, ..., N_s - 1, \\ v_i &: i = 0, 1, ..., M - 1. \end{aligned} \tag{5}$$

Here N_s is the number of 2D radial slices and M is the number of points sampled along the segmented boundary. The 3D mesh is constructed using triangles by connecting adjacent nodes in U and V directions as shown in Fig. 3(b). The result is a smooth 3D mesh structure representing the ovarian surface (see Fig. 3(c)).

3. EXPERIMENTAL RESULTS

To classify the performance of our algorithm pipeline, we use two datasets (training and validation) acquired using WS80A (Samsung Medison) ultrasound equipment equipped with an endovaginal probe V5-9. The U-Net training weights are calculated using training dataset comprising of 1500 2D slice extracted from 50 TVUS volumes.

A set of 55 TVUS volumes is used to generate validation dataset. For each of 55 volumes, ovarian volume was manually estimated using VOCAL by an expert using 5D Viewer^{TM} software [3]. The qualitative results of the segmentation framework are presented in Fig. 4. The complex and heterogeneous ovarian boundary is accurately segmented in the images shown. The hybrid segmentation approach yielded an enhancement with respect to segmentation accuracy compared to a thresholded deep learned energy map P_L as can be seen in Fig. 4. Quantitatively, we observe approximately 86% average Dice overlap with the ground truth annotations.

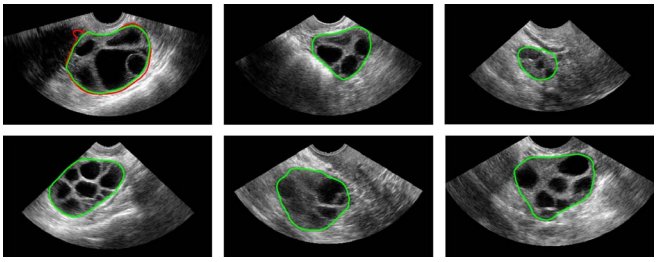

Fig. 4. Segmentation results are shown in green. The red contour shows the output of thresholded deep learned energy map.

We evaluate the performance of our algorithm by comparing the volume measurement between our algorithm and state-of-the-art VOCAL technique. Fig 5 illustrates qualitative comparison between surface mesh generated using VOCAL and automated method. The automated method generates surface mesh which is smooth and with less interpolation error as compared to VOCAL. Fig. 6 shows the comparison of measurements obtained from the manual VOCAL technique and from the automated one. Fig. 6 indicates a good agreement (Pearson Coefficient 0.92) between the measures using VOCAL and those obtained from the automated method. The mean absolute volume error over 55 volumes was found to be 4.95cm^3 with a standard deviation of 5.36. In general, the

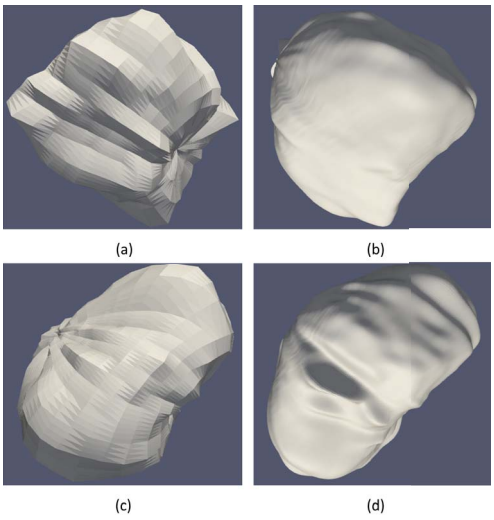

Fig. 5. Mesh visualization. (a, c): VOCAL; (b, d): Automated

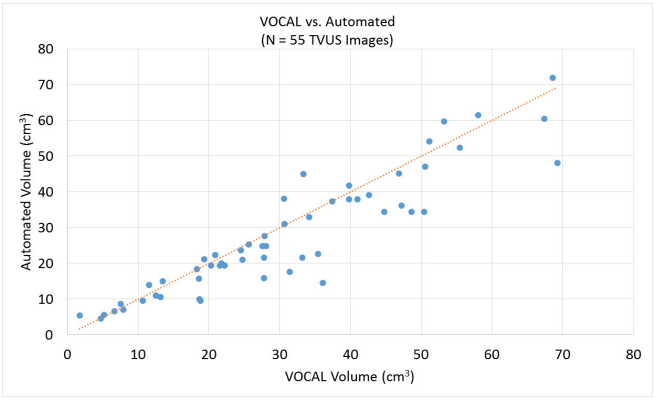

Fig. 6. Scatter plot of ovarian volume measurement using VOCAL and automated methods (Pearson Coefficient $r = 0.92$).

volume measurements using automated method were found to be less than the VOCAL measurements. Additionally, the segmented ovarian boundary helps in reducing the number of non-ovarian objects and preventing follicle bleeding. An example of this is shown in Fig. 7.

4. DISCUSSION AND CONCLUSION

The proposed algorithm pipeline addresses the problem of ovarian quantification in routine gynecological examination and automating the ovarian volume measurement in three-dimensional TVUS images. Automated ovarian volume measurement using the proposed algorithm pipeline is shown feasible. The algorithm has good agreement (Pearson Coefficient 0.92) with VOCAL. Furthermore, our proposed method could be generalized to segment other organs such as gestational

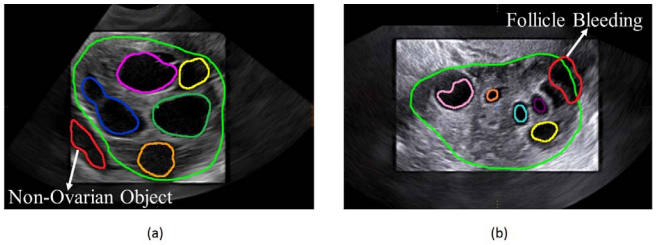

Fig. 7. (a) Non-ovarian object classification; (b) Follicle bleeding

sac, uterus, etc. Future work includes developing a tracking framework for ovarian volume registration during in-vitro fertilization cycle.

5. REFERENCES

[1] Thomas W. Kelsey et al., "Ovarian volume throughout life: a validated normative model," *PloS one*, vol. 8, no. 9, pp. e71465, 2013.

[2] Thomas W Kelsey and W Hamish B Wallace, "Ovarian volume correlates strongly with the number of nongrowing follicles in the human ovary," *Obstetrics and gynecology international*, vol. 2012, 2012.

[3] "Samsung Healthcare," http://www.samsunghealthcare.com/en/.

[4] J. P. Kusanovic et al., "The use of inversion mode and 3D manual segmentationin volume measurement of fetal fluid-filled structures:comparison with virtual organ computer-aided analysis(VOCAL)," *Ultrasound Obstet Gynecol*, vol. 31, pp. 177–186, 2008.

[5] T. Chen et al., "Automatic ovarian follicle quantification from 3D ultrasound data using global/local context with database guided segmentation," in *IEEE ICCV*, Sept 2009, pp. 795–802.

[6] Cigale B., Leni M., and Zazula D., "Segmentation of ovarian ultrasound images using cellular neural networks trained by support vector machines," *Lecture Notes in Computer Science*, vol. 4253, 2006.

[7] S. Mukherjee and S. T. Acton, "Region based segmentation in presence of intensity inhomogeneity using legendre polynomials," *IEEE Signal Processing Letters*, vol. 22, no. 3, pp. 298–302, 2015.

[8] V. Caselles et. al., "Geodesic active contours," *International Journal of Computer Vision*, vol. 22, no. 1, pp. 61–79, 1997.

[9] Yann LeCun, "Convolutional nets and cifar-10: An interview with Yann LeCun," 2014.

[10] O. Ronneberger et al., "U-Net: Convolutionalnetworks for biomedical image segmentation," *MICCAI*, pp. 234–241, 2015.